Setup and Validation of a $P\rho T$ Measuring Device. Volumetric Behavior of the Mixture 1,8-Cineole + Ethanol

José M. Lasarte, Luis Martín, Elisa Langa, José S. Urieta, and Ana M. Mainar*

Group of Applied Thermodynamics and Surfaces (GATHERS), Aragon Institute for Engineering Research (I3A), Facultad de Ciencias, Universidad de Zaragoza, Zaragoza 50009, Spain

A measuring device, based on the vibrating tube principle, for measuring $P\rho T$ data is described. The device was checked against the recommended literature values of the 1-hexanol + *n*-hexane binary system within the temperature and pressure ranges (278.15 to 313.15) K and (0.1 to 20) MPa. The relative deviations between experimental and bibliographic densities are lower than 0.2 %. After the validation, the original mixture 1,8-cineole + ethanol was studied in the ranges (283.15 to 313.15) K and (0.1 to 20) MPa. The isothermal compressibility, the isobaric thermal expansion, and the excess molar volume were derived from the experimental density data, revealing that a volume contraction occurs for this binary system. Four different equations of state, Peng–Robinson, Sako−Wu−Prausnitz, Statistical Associating Fluid Theory (SAFT), and Perturbed-Chain Statistical Associating Fluid Theory (PC-SAFT), were applied to predict the volumetric behavior of the ethanolic mixture. The best predictions were achieved with the PC-SAFT equation of state.

Introduction

Experimental knowledge of thermophysical properties of organic liquids and their mixtures presents great interest for both industrial and theoretical purposes. Information about pressure and temperature dependencies of such properties allows thermodynamic modeling based on equations of state and statistical mechanics to be checked. The rationalization of high-pressure methods permits the development of green, environment-friendly processes, which are being applied successfully. In this context, considering the importance of the $P\rho T$ data, a device for its measure was implemented.[1,2] It is based on a vibrating tube densimeter, and it is able to measure densities over broad temperature and pressure ranges. The experimental equipment as well as the experimental procedure will be described in detail.

The present work was carried out in three different stages. The first step involved the design and construction of an effective and low-cost sampling−pressurizer system that could work coupled to a commercial high-pressure densimeter. After that, the reliability of the proposed device was checked. For this purpose, the standard binary system 1-hexanol + *n*-hexane was selected.[3–7] Finally, an original mixture of our interest was studied.

The selected binary mixture is made up of 1,3,3-trimethyl-2-oxabicyclo[2.2.2]octane, also known as eucalyptol or 1,8-cineole, and ethanol. Both solvents are considered as friendly compounds in a green chemistry context with wide a variety of applications (pharmacology,[8,9] biology,[10] agriculture,[11] and energy,[12] among others). The mixture 1,8-cineole + ethanol shows a potential industrial application because of its interest in greener processes like essential oil extraction with supercritical fluids.[13] The pressure and temperature ranges of measurement [(0.1 to 20) MPa and (283.15 to 313.15) K] were selected due to the experimental conditions employed in our laboratory[14] when extracting volatile oils containing 1,8-cineole using supercritical CO_2 and alcohols as entrainers. The study also includes isobaric thermal expansivities and isothermal compressibilities, as well as the excess volumes.

Besides the experimental data, the modeling of the thermophysical properties is the nexus between the fundamental knowledge and its later application to develop industrial processes. To this extent, four equations of state, as predictive, were tested: Peng–Robinson (PR),[15] Sako−Wu−Prausnitz (SWP),[16,17] the Statistical Associating Fluid Theory (SAFT),[18–20] and the Perturbed-Chain Statistical Associating Fluid Theory (PC-SAFT).[21,22]

Experimental Section

Chemicals and Preparation of Samples. *n*-Hexane (purity, mole fraction > 99.5 %) and 1-hexanol (purity, mole fraction > 99 %) were supplied from Panreac and 1,8-cineole (purity, mole fraction > 99 %) and ethanol (purity, mole fraction > 99.8 %) from Aldrich and Scharlab, respectively. The stated purities of the chemicals were checked by gas chromatographic analysis. All liquids were used without further purification.

Mixtures were set by weighing on a Mettler Toledo AB265-S balance, whose precision is $\pm 10^{-2}$ kg. They were prepared in 11 mL airtight glass vials. The uncertainty in the mole fraction was ± 0.0001.

Experimental Device. A schematic view of the experimental device, similar to others previously used by Sousa et al.[23] and Esteve et al.,[24] is presented in the Supporting Information, Figure S1. A detailed description of the apparatus, together with the setup and validation of the equipment, is also included in the Supporting Information.

The measuring principle lays on the determination of the oscillation period of a U-shaped tube that contains the sample. The uncertainty in the control of the temperature is ± 0.01 K. The pressure of the system was controlled by two pressure transmitters (STW-A09), with ± 0.1 % full-scale uncertainty of measurement, one operating up to 16 MPa and the other up to 70 MPa.

* Corresponding author. E-mail: ammainar@unizar.es. Fax: +34 976 761 202. Phone: +34 976 761 200.

10.1021/je800024u CCC: $40.75
Published on Web 05/01/2008

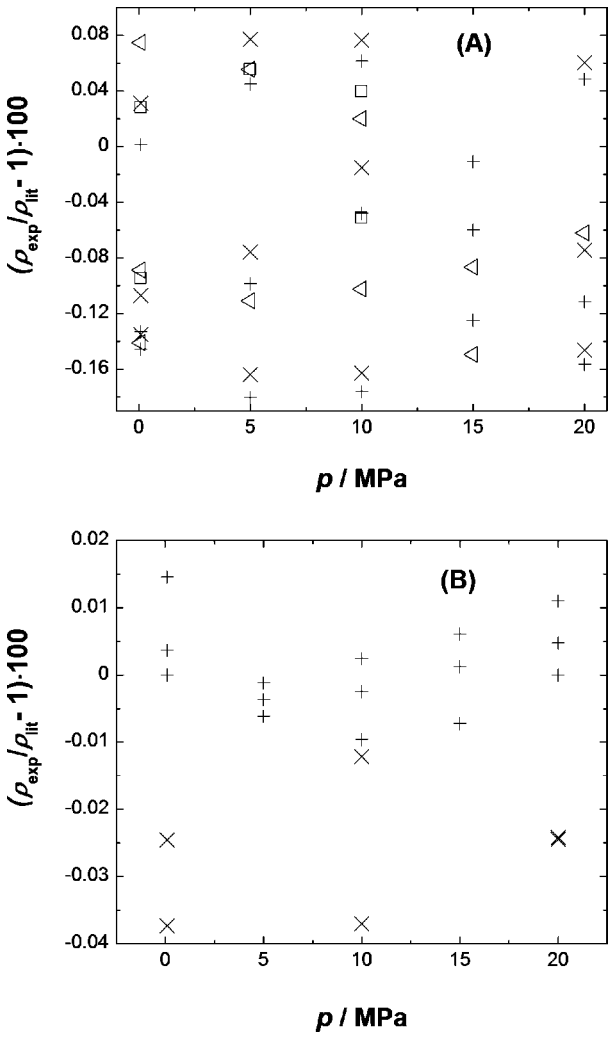

Figure 1. Comparison of densities for pure compounds vs pressure shown as deviation ($\rho_{exptl}/\rho_{lit.} - 1$) between experimental values of this work and literature values. (A) Differences for *n*-hexane: open triangle pointing left, by NIST[25] at (283.15, 298.15, and 313.15) K; □, by Sauermann et al.[27] at (298.15 and 313.15) K; +, by Troncoso et al.[3] at (283.15, 298.15, and 313.15) K; ×, by TRC[26] at (283.15, 298.15, and 313.15) K. (B) Differences for 1-hexanol: +, by Troncoso et al.[3] at (283.15, 298.15, and 313.15) K; ×, by TRC[28] at (283.15 and 313.15) K.

The evaluation of the equipment was accomplished by using two calibrating fluids, water (Milli-Q quality) and *n*-octane (purity, mole fraction > 99.5 %). The liquids were degassed before use. By applying the law of propagating errors, the overall experimental uncertainty in the reported density values was estimated to be ± 0.5 kg·m^{-3}.

The validation of the device was done by measuring the densities of the *n*-hexane + 1-hexanol mixtures at (278.15 to 313.15) K and (0.1 to 20) MPa. The experimental results are gathered in the Supporting Information (Table S1). Figures 1 and 2 show, respectively, the relative deviation between bibliographic and experimental data for the pure compounds[3,25–28] and for the *n*-hexane + 1-hexanol mixtures.[3] The obtained results revealed an adequate accuracy of our data.

Results

Densities. Once the device was calibrated and validated, experimental densities, ρ, for pure liquids and binary mixtures 1,8-cineole + ethanol were measured at three temperatures,

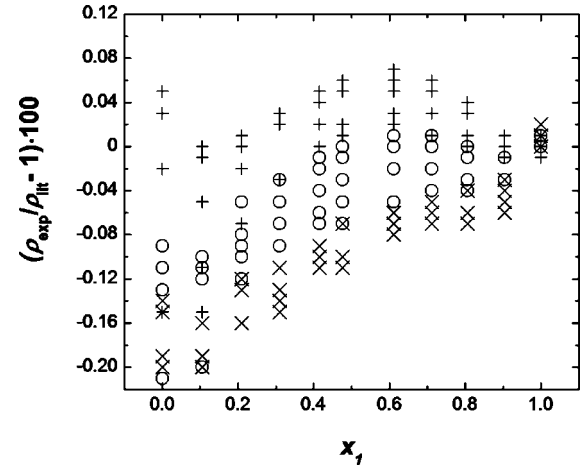

Figure 2. Comparison of densities for 1-hexanol (1) + *n*-hexane (2) vs mole fraction shown as deviation ($\rho_{exptl}/\rho_{lit} - 1$) between experimental values of this work and interpolated values from Troncoso et al.[3] at (0.1, 5, 10, 15, and 20) MPa: ×, 283.15 K; ○, 298.15 K; +, 313.15 K.

Table 1. Density, ρ, as a Function of Temperature, Pressure, and Mole Fraction for Mixtures 1,8-Cineole (1) + Ethanol (2)

	ρ/kg·m^{-3}				
	P/MPa				
x_1	0.1	5	10	15	20
	T/K = 283.15				
0	797.9	802.0	805.9	809.7	813.4
0.0983	833.3	837.2	841.0	844.5	848.0
0.1991	858.9	862.6	866.2	869.7	873.0
0.2954	877.2	880.8	884.2	887.7	891.0
0.3901	891.1	894.6	898.0	901.4	904.7
0.4930	902.9	906.4	909.7	913.0	916.2
0.5980	912.3	915.8	919.1	922.3	925.5
0.6981	919.3	922.8	926.0	929.3	932.4
0.7967	924.9	928.3	931.5	934.7	937.8
0.8898	929.2	932.7	935.9	939.0	942.1
1	933.3	936.7	939.9	943.1	946.2
	T/K = 298.15				
0	784.9	789.3	793.7	797.8	801.5
0.0983	819.9	823.9	828.1	832.0	835.5
0.1991	845.7	849.7	853.7	857.5	861.0
0.2954	864.3	868.1	872.0	875.7	879.1
0.3901	878.2	882.0	885.7	889.4	892.7
0.4930	889.9	893.7	897.4	901.1	904.3
0.5980	899.3	903.1	906.7	910.3	913.5
0.6981	906.4	910.2	913.8	917.3	920.4
0.7967	912.1	915.8	919.3	922.7	925.9
0.8898	916.4	920.1	923.6	927.1	930.2
1	920.4	924.1	927.7	931.2	934.4
	T/K = 313.15				
0	772.0	777.0	781.5	786.0	790.1
0.0983	807.2	812.0	816.3	820.7	824.7
0.1991	832.7	837.3	841.5	845.7	849.5
0.2954	851.2	855.6	859.7	863.8	867.5
0.3901	865.0	869.4	873.4	877.4	881.1
0.4930	876.8	881.0	884.9	888.9	892.5
0.5980	886.2	890.4	894.2	898.1	901.7
0.6981	893.3	897.5	901.3	905.1	908.6
0.7967	898.8	902.9	906.7	910.6	914.1
0.8898	903.2	907.3	911.0	914.8	918.3
1	907.3	911.4	915.2	919.0	922.5

(283.15, 298.15, and 313.15) K, and several pressures from (0.1 to 20) MPa in steps of 5 MPa. The experimental results appear in Table 1.

Figure 3 shows the relative deviation between experimental and bibliographic data for ethanol[27–32] (< 0.1 %) and 1,8-cineole[33–35] (< 0.2 %). Figure 4 includes the relative deviations at 0.1 MPa for the binary mixture between our

Table 2. Fitting Coefficients of Equation 1 for the Pure Liquids and Mixtures 1,8-Cineole (1) + Ethanol (2) and Standard Deviations s[a]

	$x_1 = 0$	$x_1 = 0.0983$	$x_1 = 0.1991$	$x_1 = 0.2954$	$x_1 = 0.3901$	$x_1 = 0.4930$
a_0/kg·m^{-3}	806.475	841.871	867.548	885.836	899.763	911.613
a_1/kg·m^{-3}·K^{-1}	−0.8617	−0.8699	−0.8715	−0.8644	−0.8665	−0.8698
b_0/MPa	76.6	75.6	86.6	102.4	103.4	105.1
b_1/MPa·K^{-1}	−0.459	0.330	−0.396	−0.622	−0.627	−0.896
b_2/MPa·K^{-2}	–	−1.7E−02	−3.2E−03	–	–	5.4E−03
c_0	0.0781	0.0764	0.0750	0.0823	0.0803	0.0773
s/kg·m^{-3}	0.08	0.16	0.08	0.08	0.08	0.07

	$x_1 = 0.5980$	$x_1 = 0.6981$	$x_1 = 0.7967$	$x_1 = 0.8898$	$x_1 = 1$
a_0/kg·m^{-3}	921.027	927.981	933.689	937.981	941.985
a_1/kg·m^{-3}·K^{-1}	−0.8698	−0.8654	−0.8698	−0.8678	−0.8658
b_0/MPa	99.6	84.0	106.2	95.2	103.0
b_1/MPa·K^{-1}	−0.749	−0.659	−0.955	−0.882	−0.964
b_2/MPa·K^{-2}	3.3E−03	3.5E−03	6.2E−03	6.7E−03	7.2E−03
c_0	0.0728	0.0613	0.0731	0.0658	0.0707
s/kg·m^{-3}	0.07	0.09	0.13	0.10	0.09

[a] $s = \sqrt{\sum_{i=1}^{N} (\rho_{i,\mathrm{exptl}} - \rho_{i,\mathrm{calcd}})^2/(N-P)}$; where N = number of experimental points and P = number of adjustable parameters.

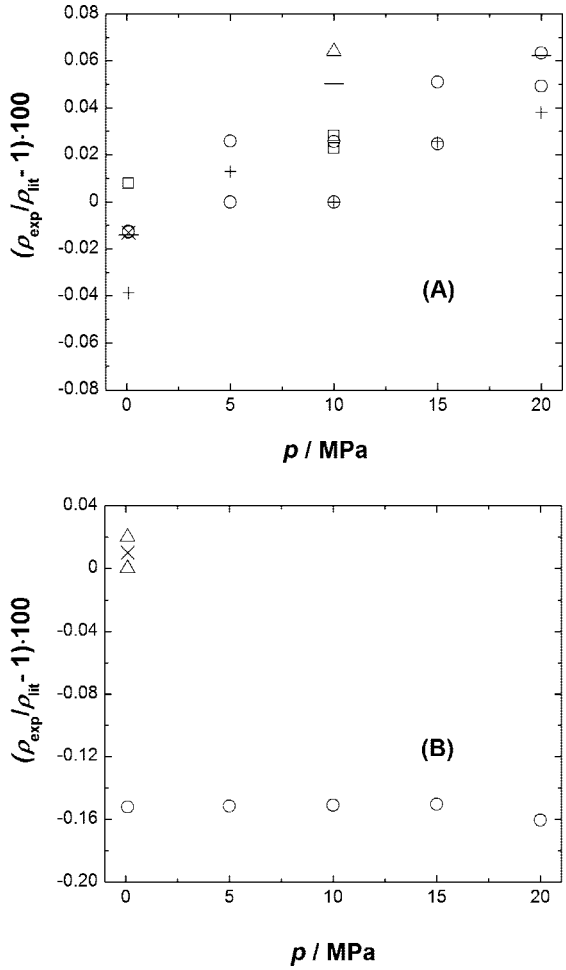

Figure 3. Comparison of densities for pure compounds vs pressure shown as deviation ($\rho_{\mathrm{exptl}}/\rho_{\mathrm{lit}} - 1$) between experimental values of this work and literature values. (A) Differences for ethanol: △, by Cibulka et al.[31] at 313.15 K; —, by TRC[30] at 298.15 K; +, by Watson et al.[32] at 313.15 K; ○, by Zeberg et al.[29] at (283.15 and 313.15) K; □, by Sauermann et al.[27] at (298.15 and 313.15) K; ×, by Sharma et al.[35] at 313.15 K. (B) Differences for 1,8-cineole: △, by Alfaro et al.[34] at (298.15 and 313.15) K; ○, by Aparicio et al.[33] at 298.15 K; ×, by Sharma et al.[35] at 313.15 K.

experimental results and the interpolated values from Alfaro et al.[34] (vibrating method, DMA 58) and Sharma et al.[35] (pycnometric method). The absolute differences are lower than 0.2 % and 0.6 %, respectively.

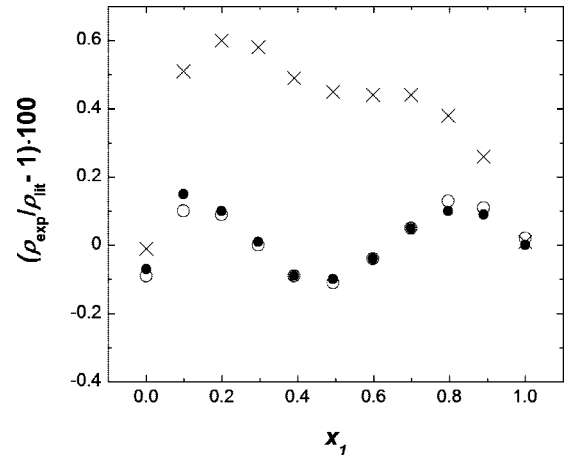

Figure 4. Comparison of densities for 1,8-cineole (1) + ethanol (2) vs mole fraction shown as deviation ($\rho_{\mathrm{exptl}}/\rho_{\mathrm{lit}} - 1$) between experimental values of this work and interpolated values at 0.1 MPa from Alfaro et al.:[34] ○, 298.15 K; ●, 313.15 K; and from Sharma et al.:[35] ×, 313.15 K.

For each composition, the compressed liquid densities were correlated with the modified Tait relationship[36]

$$\rho(P,T)/\mathrm{kg\cdot m^{-3}} = \rho(0.1,T)/\mathrm{kg\cdot m^{-3}}\left(1 - C(T)\ln\frac{B(T)/\mathrm{MPa} + P/\mathrm{MPa}}{B(T)/\mathrm{MPa} + 0.1/\mathrm{MPa}}\right)^{-1} \quad (1)$$

where $C(T)$ and $B(T)$ are temperature-dependent functions. In this work, the following expression for B is used

$$B/\mathrm{MPa} = b_0 + b_1(T - T_0/\mathrm{K}) + b_2(T - T_0/\mathrm{K})^2 \quad (2)$$

and C is assumed to be temperature independent. $\rho(0.1, T)$ is the density at 0.1 MPa, interpolated by the following correlation

$$\rho(0.1,T)/\mathrm{kg\cdot m^{-3}} = a_0 + a_i(T - T_0/\mathrm{K}) \quad (3)$$

where $T_0 = 273.15$ K in all cases. The coefficients were obtained using the Marquardt algorithm and are given in Table 2 along with the standard deviation for each composition. Figure 5 presents the experimental density and the fitted surface of 1,8-cineole (1) + ethanol (2) vs x_1 and P at 298.15 K.

Derived Properties: Isobaric Thermal Expansivity, α_P, Isothermal Compressibility, κ_T, and Excess Molar Volume, V_m^E. Differentiating eq 1 with respect to temperature and pressure, the isobaric thermal expansivity, α_P, and the isothermal

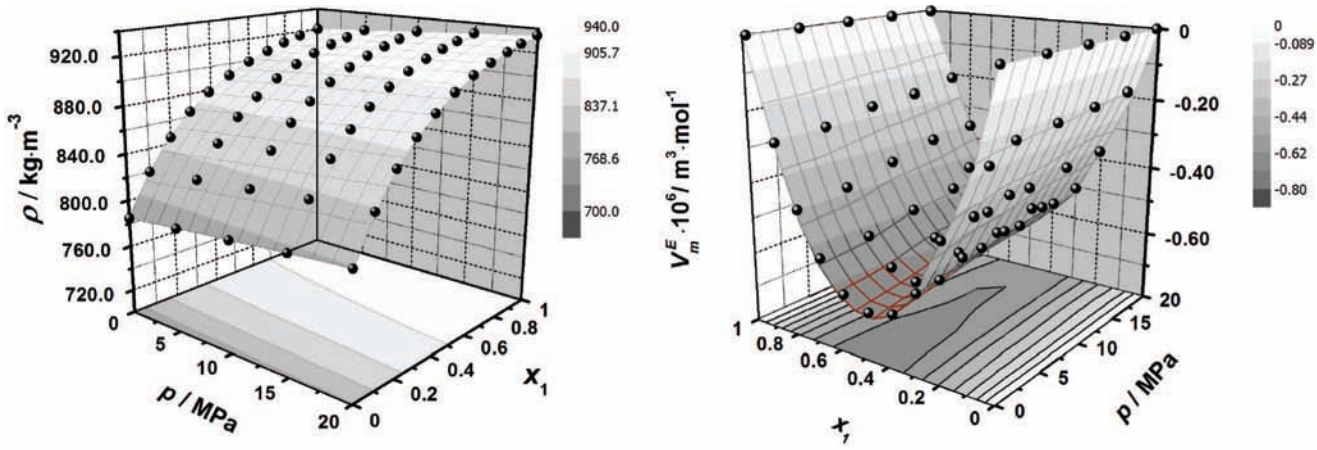

Figure 5. Experimental density, ρ, excess molar volume, $V^{\mathrm{E}}_{\mathrm{m}}$, and fitted surfaces for the mixture 1,8-cineole (1) + ethanol (2) vs mole fraction and pressure at 298.15 K. Contour plots appear at the bottom of the figure.

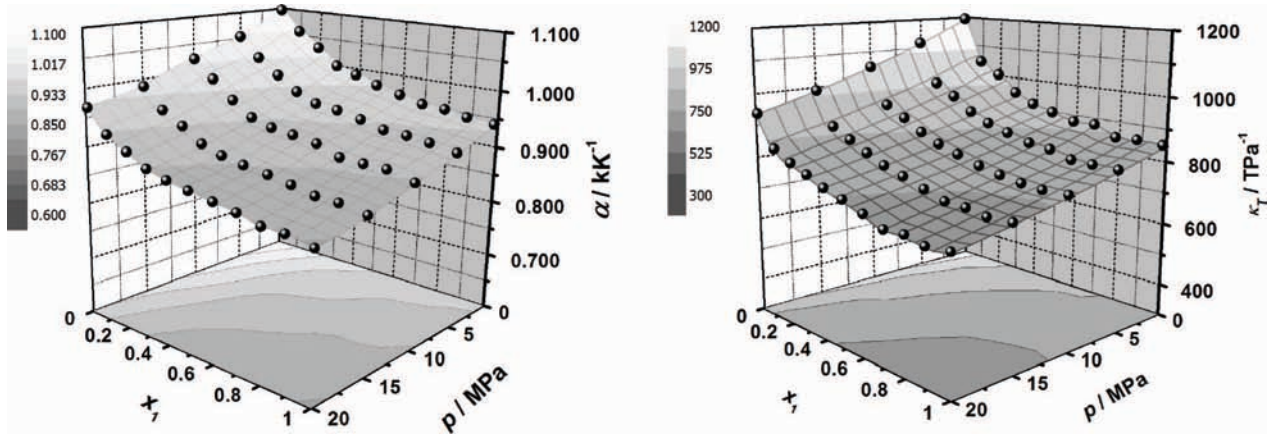

Figure 6. Calculated isobaric thermal expansivity, α_P, and calculated isothermal compressibility, κ_T, for the mixture 1,8-cineole (1) + ethanol (2) vs mole fraction and pressure at 298.15 K. Contour plots appear at the bottom of the figure.

compressibility, κ_T, can be evaluated taking into account their definition:

$$\alpha_P = -\frac{1}{\rho}\left(\frac{\partial \rho}{\partial T}\right)_P \tag{4}$$

$$\kappa_T = \frac{1}{\rho}\left(\frac{\partial \rho}{\partial P}\right)_T \tag{5}$$

It is well-known[37] that analytical differentiation of the Tait equation with respect to pressure is certainly the most direct way to obtain reliable isothermal compressibility data.

$$\kappa_T/\mathrm{MPa}^{-1} = \frac{C \cdot [B(T)/\mathrm{MPa} + P/\mathrm{MPa}]}{1 - C \cdot \ln[(B(T)/\mathrm{MPa} + P/\mathrm{MPa})/(B(T)/\mathrm{MPa} + 0.1/\mathrm{MPa})]} \tag{6}$$

The calculated isothermal compressibilities were estimated to have an expanded uncertainty of ± 14 TPa^{-1}.

In a similar way, isobaric thermal expansivity data can be determined from analytical calculation. But as Cerdeiriña et al.[38] and Troncoso et al.[3] mention, the estimated isobaric thermal expansivities depend highly on the applied temperature-dependent functions for B and $\rho(0.1, T)$. Because of this, they recommend to derive the isobaric thermal expansivity numerically from the density values at constant pressure. α_P was evaluated in the investigated pressure and temperature ranges finding an expanded uncertainty of ± 0.005 $\mathrm{k \cdot K^{-1}}$. The calculated values of κ_T and α_P are given in Table S2 of Supporting Information. Figure 6 shows the calculated values of these properties for the 1,8-cineole (1) + ethanol (2) mixture vs x_1 and P at 298.15 K.

For all compositions within the considered T, P range, the isothermal compressibility, as well as the isobaric thermal expansion, increases with increasing temperature and decreases with increasing pressure. Within the considered T, P conditions, it is observed that ethanol is more compressible and expansive than 1,8-cineole. Both properties show a monotonically decreasing behavior as a function of the 1,8-cineole concentration. Taken the x-axis as reference, the convex-shape found for κ_T and α_P vs x_1 (logical consequence of the dependence between the density of the mixture with the composition) could be explained as the result of a decrease in the free volume of the molecules within the mixtures.

Excess molar volumes as a function of 1,8-cineole molar fraction, x_1, were determined at each P, T from densities of the two pure liquids, ρ_1 and ρ_2, and from that of their mixtures, ρ, according to the relation

$$V^{\mathrm{E}}_{\mathrm{m}}(P,T) = x_1 M_1\left(\frac{1}{\rho} - \frac{1}{\rho_1}\right) + x_2 M_2\left(\frac{1}{\rho} - \frac{1}{\rho_2}\right) \tag{7}$$

where M_1 and M_2 are the molar masses of 1,8-cineole and ethanol, respectively. The calculated values obtained by eq 7

Table 3. Fitting Coefficients of Equation 8 for the Mixture 1,8-Cineole (1) + Ethanol (2) and Standard Deviations s at the Given (P, T) Conditions[a]

	P/MPa				
	0.1	5	10	15	20
		T/K = 283.15			
$A_1 \cdot 10^6/m^3 \cdot mol^{-1}$	−2.646	−2.539	−2.490	−2.448	−2.369
$A_2 \cdot 10^6/m^3 \cdot mol^{-1}$	−0.128	−0.052	−0.046	−0.091	−0.090
$A_3 \cdot 10^6/m^3 \cdot mol^{-1}$	–	−0.161	–	–	–
$s \cdot 10^6/m^3 \cdot mol^{-1}$	0.009	0.011	0.012	0.010	0.011
		T/K = 298.15			
$A_1 \cdot 10^6/m^3 \cdot mol^{-1}$	−2.746	−2.658	−2.549	−2.500	−2.411
$A_2 \cdot 10^6/m^3 \cdot mol^{-1}$	−0.016	0.088	−0.012	−0.045	−0.109
$A_3 \cdot 10^6/m^3 \cdot mol^{-1}$	–	0.118	0.144	0.277	0.336
$s \cdot 10^6/m^3 \cdot mol^{-1}$	0.015	0.016	0.016	0.017	0.014
		T/K = 313.15			
$A_1 \cdot 10^6/m^3 \cdot mol^{-1}$	−2.806	−2.711	−2.622	−2.566	−2.485
$A_2 \cdot 10^6/m^3 \cdot mol^{-1}$	−0.130	−0.162	−0.212	−0.213	−0.221
$s \cdot 10^6/m^3 \cdot mol^{-1}$	0.013	0.014	0.012	0.012	0.014

[a] $s = \sqrt{\sum_{i=1}^{N} (V^E_{mi,exptl} - V^E_{mi,calcd})^2/(N-P)}$; where N = number of experimental points and P = number of adjustable parameters.

Table 4. Pure Component Properties Used for the Application of the Equations of State

compound	M_w / g·mol^{-1}	T_c / K	P_c / MPa	T_b / K	ω
ethanol[a]	46.096	513.90	61.48	351.4	0,644
1,8-cineole	154.249	661.12[b]	30.19[b]	449.60[c]	0,338[d]

[a] Ref 52. [b] Calculated using Joback's method, ref 40. [c] Ref 43. [d] Calculated using the Lee−Kesler method, ref 41.

Table 5. Pure Component Parameters Used for the Application of the Studied Equations of State

SWP	v^{00}/L·mol^{-1}	c
ethanol	2.39507	0.357191
1,8-cineole	1.27558	0.354786

SAFT	m	v^{00}/L·mol^{-1}	u^0/k/K	κ	ϵ/k/K
ethanol[18]	2.457	0.0120	213.48	0.02920	2759
1,8-cineole	17.866	4.819	264.24	–	–

PC-SAFT	m_i	σ_i/Å	ϵ_i/k/K	$\kappa^{A_iB_i}$	$\epsilon^{A_iB_i}/k$/K
ethanol[22]	2.3827	3.1771	198.24	0.032384	2653.3
1,8-cineole	4.1640	3.1979	302.86	–	–

Table 6. Absolute Average Percentage Deviation, AAD %, for the Correlation of Saturation Properties and Prediction of Compressed Liquid Density[a]

compound	EOS	AAD % P^{sat}	AAD % ρ^{sat}	ΔT_c/K	ΔP_c/MPa	AAD % ρ^{comp}
1,8-cineole	PR	2.75	6.91			6.07
	SWP	8.23	0.53			0.30
	SAFT	3.33	2.55	30.78	0.24	3.86
	PC-SAFT	2.84	0.15	35.88	0.32	0.53
ethanol	SWP	1.21	18.45			0.69

[a] AAD % = $100/N \cdot \Sigma|\rho_{i,EOS} - \rho_{i,exptl}|/\rho_{i,exptl}$, where N = number of points; $\Delta T_c = T_{c,EOS} - T_c$; and $\Delta P_c = P_{c,EOS} - P_c$.

appear in Table S3 of the Supporting Information. The estimated uncertainty on V^E_m is $\pm 5 \cdot 10^{-8}$ m^3·mol^{-1}. This excess quantity was fitted to the Redlich–Kister equation

$$V^E_m(P,T)/m^3 \cdot mol^{-1} = x_1 x_2 (A_1 + A_2(1-2x_1) + A_3(1-2x_1)^2) \quad (8)$$

where x_1 and x_2 are the molar fractions of 1,8-cineole and ethanol, respectively, and A_i are the fitting parameters. The values of the A_i parameters and the standard deviations are shown in Table 3.

The variation of the excess molar volume and the fitted surface versus the composition of 1,8-cineole and pressure is shown at 298.15 K in Figure 5. For all the mixtures in the whole T, P range, this magnitude is negative indicating that this mixture is better packed than the pure compounds.

Taking into account its uncertainty, the dependence of V^E_m with temperature is negligible. This behavior was previously described by Alfaro et al.[34] (1,8-cineole + ethanol) and Vallés et al.[39] (2-methyltetrahydrofuran + 1-butanol) at atmospheric pressure. Following the heat of mixing reported by Alfaro et al.[34] ($\approx$ 300 J·mol^{-1}), we can state that this is not a very usual behavior for a mixture. Commonly, the breaking of association (ethanol) produces an expansion of the mixture as the intermolecular distance grows with less or weaker interaction. The obtained values for the excess molar volumes would indicate that the molecules of 1,8-cineole and ethanol intertwine occupying more effectively than expected for a given volume.

At 1 bar, the mentioned intertwining between 1,8-cineole and ethanol would be a consequence of the ether−alcohol interactions (remember the slight endothermic nature of the mixture, $\approx$ 300 J·mol^{-1}). When pressure increases, a loosening of the molecular packing and an enlargement of the free volume are produced.

Equations of State (EOS). Four EOS were tested in this work to predict the $P\rho T$ behavior of the fluid mixtures. Two of them are cubic equations put forward by Peng–Robinson (PR)[15] and Sako−Wu−Prausnitz (SWP),[16,17] and the other two are based on the theory of perturbations: the Statistical Associated Fluid Theory (SAFT, Huang and Radosz's version)[18–20] and the Perturbed Chain-Statistical Associated Fluid Theory (PC-SAFT).[21,22] The needed properties of the pure components are gathered in Table 4. Critical properties of 1,8-cineole were calculated according to Joback's method[40] and the acentric factor was estimated using the Lee-Kesler method.[41] The needed EOS parameters for 1,8-cineole were evaluated from the correlation of vapor pressure properties[42,43] and liquid densities extrapolated by eq 1. The additional SWP parameters of ethanol were also obtained from correlation of the saturated properties given by Daubert and Danner.[44]

Cubic EOS. To a first stage, the SWP EOS was applied to obtain the pure components parameters that appear in Table 5. The AAD % values for the compressed densities of the two pure liquids are shown in Table 6. The SWP EOS yielded lower

deviations (0.30 %) than PR EOS (6.07 %). To determine the $P\rho T$ behavior of 1,8-cineole + ethanol mixtures, the van der Waals one-fluid mixing rules were used, eqs 9 and 10

$$a = \sum_{i=1}^{N}\sum_{j=1}^{N} x_i x_j a_{ij} \tag{9}$$

$$b = \sum_{i=1}^{N}\sum_{j=1}^{N} x_i x_j b_{ij} \tag{10}$$

In this work the classical quadratic combining rule for the cross-terms a_{ij} and b_{ij} was selected

$$a_{ij} = \sqrt{a_i a_j}(1 - k_{ij}) \tag{11}$$

$$b_{ij} = \frac{b_i + b_j}{2}(1 - l_{ij}) \tag{12}$$

The c parameter, as indicated by Pfohl et al.,[45] was taken as the arithmetical mean of c_i and c_j

$$c = \frac{c_i + c_j}{2} \tag{13}$$

to test the models as predictive, and the interaction parameters k_{ij} and l_{ij} were considered equal to zero.

The obtained results with PR and SWP EOS are listed in Table S4. Despite the good approach achieved with the SWP EOS for the densities of the pure compounds, the AAD % between experimental densities and the predicted values with PR are lower for the binary mixtures (2.81 % vs 4.32 %).

Equations Based on the Perturbations Theory. As it is known, the above cubic EOS are variations of the van der Waals equation, and this approach is not fully adequate for complex fluids such as those studied in this work. Taking this into account, other models that describe more properly molecular shape and intermolecular association were tested. For this purpose, the Statistical Associating Fluid Theory (SAFT)[18–20] and one of its recent modifications, the Perturbed-Chain Statistical Associating Fluid Theory (PC-SAFT),[21,22] were chosen. The SAFT-based models develop a molecularly founded equation using rigorous statistical mechanics. In these models, the component molecules are described as chains of segments, and the residual Helmholtz energy is regarded as the sum of a main reference contribution and a minor dispersive perturbation. The reference term includes the hard-sphere, chain, and association terms, according to eq 14.

$$a = a^{\text{ref}} + a^{\text{disp}} = a^{\text{hs}} + a^{\text{chain}} + a^{\text{assoc}} + a^{\text{disp}} \tag{14}$$

The most important difference between SAFT and PC-SAFT is the way in which the reference fluid is described. In this work, the SAFT version developed by Huang and Radosz[18–20] was applied to describe the $P\rho T$ behavior of pure and mixed solvents. This version of the SAFT equation is based on Wertheim's thermodynamic perturbation theory of first order.[46–49] Huang and Radosz applied a dispersion term developed by Chen and Kreglewski,[50] but the nonspherical shape of molecules is not accounted for in this term. On the other hand, the PC-SAFT model, developed by Gross and Sadowski,[21,22] applies the second-order perturbation theory of Barker–Henderson[51] to a hard-chain reference. For the sake of simplicity, algebraic expressions for both models are not included here. 1,8-Cineole was regarded as a nonassociating molecule (Figure S2) and ethanol as an associative molecule with two associating sites.

For describing 1,8-cineole and ethanol, three and five parameters are required, respectively, to apply the SAFT model, namely, the segment number m, the segment volume π^{00}, the segment–segment interaction energy $u°/k$, the association energy ϵ/k, and the association volume κ. The PC-SAFT equation also uses, respectively, three and five parameters to identify nonassociating and associating compounds, namely, the segment numer m_i, the segment diameter σ_i, the segment energy parameter u/k, the association energy ϵ/k, and the effective association volume $\kappa^{A_i B_i}$. The pure component parameters of 1,8-cineole were identified by simultaneously fitting vapor pressure data and liquid density data. For ethanol, these parameters were obtained from the literature.[18,22] Table 5 gathers the parameters used to apply the SAFT-based models. The AAD % values for the compressed densities of the two pure liquids are shown in Table 6. The PC-SAFT theory yielded lower deviations (0.53 %) than the SAFT model (3.86 %).

To determine the $P\rho T$ behavior of 1,8-cineole + ethanol mixtures, the van der Waals one-fluid mixing rules were used in both models. For the SAFT equation, the so-called vdW1 mixing rules were applied to the segment energy, eqs 15 to 19

$$\frac{u}{kT} = \frac{\sum_i \sum_j x_i x_j m_i m_j \left(\frac{u_{ij}}{kt}\right)(v^0)_{ij}}{\sum_i \sum_j x_i x_j m_i m_j (v^0)_{ij}} \tag{15}$$

where x_i and x_j are the mole fractions of molecules i and j, respectively, and

$$(v^0)_{ij} = \left(\frac{1}{2}\left\{(v^0)_i^{1/3} + (v^0)_j^{1/3}\right\}\right)^3 \tag{16}$$

$$u_{ij} = (1 - k_{ij})(u_i u_j)^{1/2} \tag{17}$$

where k_{ij} is an empirical binary parameter.

The mixing rule for the average segment number for mixtures m is

$$m = \sum_i \sum_j x_i x_j m_{ij} \tag{18}$$

where

$$m_{ij} = 1/2(m_i + m_j) \tag{19}$$

The PC-SAFT formulation is more complex,[22] but in brief, the a^{disp} term depends on m_i, σ_i, and ϵ_i/k as well as on the diameter and energy between unlike segments, σ_{ij} and ϵ_{ij}/k, respectively. These parameters for a pair of unlike segments are obtained by conventional Berthelot–Lorentz combining rules

$$\sigma_{ij} = 1/2(\sigma_i + \sigma_j) \tag{20}$$

$$\epsilon_{ij} = \sqrt{\epsilon_i \epsilon_j}(1 - k_{ij}) \tag{21}$$

where k_{ij} is a binary interaction parameter introduced to correct the segment–segment interactions of unlike chains.

In our case, a binary mixture composed of a nonassociating compound and one associating compound, no mixing rules were required in the associating term, a^{assoc}.

To test both models in a predictive way, the binary interaction parameters k_{ij} were considered equal to zero.

The obtained results with SAFT and PC-SAFT EOS are listed in Table S5. The best results for the predictions of experimental compressed densities of the binary mixture under study were achieved with PC-SAFT (AAD % = 0.29 %). As a comparison, Figure 7 shows the density predictions ($k_{ij} = 0$ and $l_{ij} = 0$) of the four EOS for the densest mixture (283.15 K, 20 MPa) and the least dense mixture (313.15 K, 0.1 MPa) of 1,8-cineole + ethanol. Despite the lower AAD % found for PR (2.81 %) than

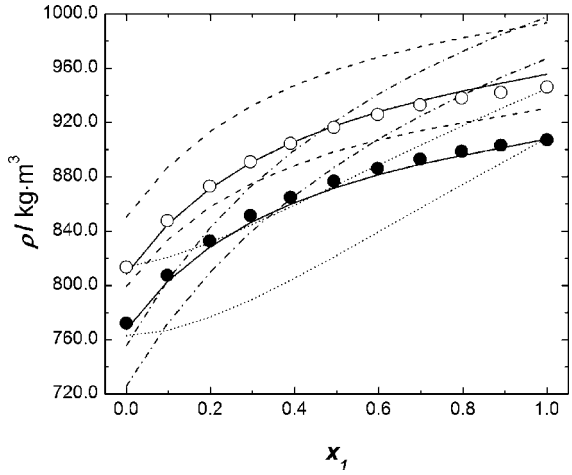

Figure 7. Density predictions of four equations of state, $k_{ij} = 0$, for the mixture 1,8-cineole (1) + ethanol (2): ○, 283.15 K and 20 MPa; ●, 313.15 K and 0.1 MPa; -•-, Peng–Robinson; - - -, SAFT; —, PC-SAFT; •••, Sako−Wu−Prausnitz.

for the SAFT equation (3.68 %), SAFT describes more adequately the behavior of the density with the mole composition of the mixture.

Conclusion

The description of a measuring system of densities for liquid and liquid mixtures over wide pressure and temperature ranges has been presented. The proposed method is found to be reliable for obtaining densities, isothermal compressibilities, isobaric thermal expansivities, and excess molar volumes, as well as their dependencies on temperature, pressure, and composition. Furthermore, the experimental density of the standard mixture *n*-hexane + 1-hexanol, the densities of 1,8-cineole and ethanol, and the density of their nine binary mixtures have been measured in the range (283.15 to 313.15) K and up to 20 MPa with an overall uncertainty of ± 0.5 kg·m^{-3}. A negative behavior of the excess molar volume versus composition is found. Four EOS, Peng–Robinson, Sako−Wu−Prausnitz, SAFT, and PC-SAFT have been tested to predict ($k_{ij} = 0$, $l_{ij} = 0$) the $P\rho T$ equilibrium of the binary system under study. The best results of the compressed densities of the mixture are obtained using PC-SAFT with an overall AAD % of 0.29 %. PC-SAFT appears as an invaluable tool to predict the $P\rho T$ behavior of the mixture 1,8-cineole + ethanol from only the VLE and the saturated density of the pure components.

Supporting Information Available:

Scheme, description, setup, and validation of the experimental device. Experimental $P\rho T$ data of the 1-hexanol + *n*-hexane mixture. Calculated values of the isothermal compressibilities, the isobaric thermal expansivities, and the excess molar volumes for the 1,8-cineole + ethanol mixture. $P\rho T$ predictions of PR, SWP, SAFT, and PC-SAFT equations of state. Molecule of 1,8-cineole. This material is available free of charge via the Internet at http://pubs.acs.org.

Literature Cited

(1) Lasarte, J. M.; Langa, E.; Pardo, J. I.; Urieta, J. S.; Mainar, A. M. Construcción y puesta a punto de un sistema a alta presión para la medida de densidades de fluidos. XXX Reunión Bienal de la Sociedad Española de Física, 2005.

(2) Lasarte, J. M. Construcción y puesta a punto de un sistema a alta presión para la medida de densidades de fluidos. Postgrado de iniciación en la investigación en áreas científicas. Universidad de Zaragoza, 2006.

(3) Troncoso, J.; Bessières, D.; Cerdeiriña, C. A.; Carballo, E.; Romaní, L. Automated Measuring Device of (p, ρ, T) Data - Application to the 1-Hexanol plus n-Hexane System. *Fluid Phase Equilib.* **2003**, *208*, 141–154.

(4) Treszczanowicz, A. J.; Treszczanowicz, T.; Benson, G. C. Review of Experimental and recommended Data for the Excess Molar Volumes of 1-Alkanol + n-Alkane Binary Mixtures. *Fluid Phase Equilib.* **1993**, *89*, 31–56.

(5) Randzio, S. L.; Grolier, J.-P. E.; Quint, J. R. Thermophysical Properties of 1-Hexanol over the Temperature Range from 303 to 503 K and at Pressures from the Saturation Line to 400 MPa. *Fluid Phase Equilib.* **1995**, *110*, 341–359.

(6) Randzio, S. L.; Grolier, J.-P. E.; Quint, J. R. Isobaric Thermal Expansivities of Binary Mixtures of n-Hexane with 1-Hexanol at Pressures from 0.1 to 350 MPa and at Temperatures from 303 to 503 K. *Int. J. Thermophys.* **1997**, *18*, 733–759.

(7) Randzio, S. L.; Grolier, J.-P. E.; Quint, J. R.; Eatough, D. J.; Lewis, E. A.; Hansen, L. D. n-Hexane as a Model for Compressed Simple Liquids. *Int. J. Thermophys.* **1994**, *15*, 415–441.

(8) Levison, K. K.; Takayama, K.; Isowa, K.; Okabe, K.; Nagai, T. Formulation Optimization of Indomethacin Gels Containing a Combination of Three Kinds of Cyclic Monoterpenes as Percutaneous Penetration Enhancers. *J. Pharm. Sci.* **1994**, *83*, 1367–1372.

(9) Heard, C. A.; Kung, D.; Thomas, C. P. Skin Penetration Enhancement of Mefenamic acid by Ethanol and 1,8-Cineole can be explained by the 'Pull' Effect. *Int. J. Pharm.* **2006**, *321* (1–2), 167–170.

(10) Gundidza, M.; Deans, S. G.; Kennedy, A. L.; Mavi, S.; Watennan, P. G.; Gray, A. L. The Essential Oil from Heteropyxis Natalensis Harv: its Antimicrobial Activities and Phyto-Constituents. *J. Sci. Food Agric.* **1993**, *63*, 361–364.

(11) Sangwan, N. K.; Verma, B. S.; Verma, K. K.; Dhindsa, K. S. Nematocidal Activity of Some Essential Plant Oils. *Pest. Sci.* **1990**, *28*, 331–335.

(12) Takeda, S.; Hoki, M. Study of Eucalyptus Oil and its Applications to Spark Ignition Engine IV. *Gakujutsu Hokoku* **1982**, *64*, 55–67.

(13) Kubat, H.; Akman, U.; Hortaçsu, Ö. Semi-Batch Packed-Column Deterpenation of Origanum Oil by Dense Carbon Dioxide. *Chem. Eng. Process* **2001**, *40*, 19–32.

(14) Langa, E. Extracción con CO_2 supercrítico de aceites esenciales de plantas aromáticas. Tesis Doctoral. Universidad de Zaragoza, 2007.

(15) Peng, D. Y.; Robinson, D. B. A new Two Constant Equation of State. *Ind. Eng. Chem. Fundam.* **1976**, *15*, 59–64.

(16) Sako, T.; Wu, A.; Prausnitz, J. M. A Cubic Equation of State for High Pressure Phase Equilibria of Mixtures Containing Polymers and Volatile Fluids. *J. Appl. Polym. Sci.* **1989**, *38*, 1839–1858.

(17) Beret, S.; Prausnitz, J. M. Perturbed Hard-Chain Theory. Equation of State for Fluids Containing Small or Large Molecules. *AIChE J.* **1975**, *21*, 1123–1132.

(18) Huang, S. H.; Radosz, M. Equation of State for Small, Large, Polydisperse and Associating Molecules. *Ind. Eng. Chem. Res.* **1990**, *29*, 2284–2294.

(19) Huang, S. H.; Radosz, M. Equation of State for Small, Large, Polydisperse and Associating Molecules: Extension to Fluid Mixtures. *Ind. Eng. Chem. Res.* **1991**, *30*, 1994–2005.

(20) Huang, S. H.; Radosz, M. Equation of State for Small, Large, Polydisperse and Associating Molecules: Extension to Fluid Mixtures (vol 30, pg 2002, 1992). *Ind. Eng. Chem. Res.* **1993**, *32*, 762.

(21) Gross, J.; Sadowski, G. Perturbed-Chain SAFT: An Equation of State Based on a Perturbation Theory for Chain Molecules. *Ind. Eng. Chem. Res.* **2001**, *40*, 1244–1260.

(22) Gross, J.; Sadowski, G. Application of the Perturbed-Chain SAFT Equation of State to Associating Systems. *Ind. Eng. Chem. Res.* **2002**, *41*, 5510–5515.

(23) Sousa, A. T.; de Castro, C. N.; Tufeu, R.; Le Neindre, B. Density of 1-Chloro-1,1-Difluoroethane (R142b). *High Temp.-High Press.* **1992**, *24*, 185–194.

(24) Esteve, X.; Conesa, A.; Coronas, A. Liquid Densities, Kinematic Viscosities, and Heat Capacities of some Alkylene Glycol Dialkyl Ethers. *J. Chem. Eng. Data* **2003**, *48*, 392–397.

(25) Lemmon, E. W.; McLinden, M. O.; Friend, D. G. Thermophysical Properties of Fluid Systems. In *NIST Chemistry WebBook, NIST Standard Reference Database Number 69*; Linstrom, P. J., Mallard, W. G., Eds.; National Institute of Standards and Technology: Gaithersburg, MD 20899, March 2003, (http://webbook.nist.gov).

(26) Tables db-1450.0 to db-1450.6. *TRC Thermodynamic Tables. Non-Hydrocarbons*; Texas A&M University: College Station, TX, 1996.

(27) Sauermann, P.; Holzapfel, K.; Oprzynski, K.; Poot, W.; de Loos, T. W. The pρT Properties of Ethanol+Hexane. *Fluid Phase Equilib.* **1995**, *112*, 249–272.

(28) Tables db-5095.0 to db-5095.1. *TRC Thermodynamic Tables. Non-Hydrocarbons*; Texas A&M University: College Station, TX, 1996.

(29) Zéberg-Mikkelsen, C. K.; Lugo, L.; García, J.; Fernández, J. Density Measurement under Pressure for the Binary System (Ethanol + Methylcyclohexane). *J. Chem. Thermodyn.* **2005**, *37*, 1294–1304.

(30) Tables db-5050.0 to db-5050.3. *TRC Thermodynamic Tables. Non-Hydrocarbons*; Texas A&M University: College Station, TX, 1995.

(31) Cibulka, I.; Ziková, M. Liquid Densities At Elevated Pressures of 1-Alkanols from C1 to C10: A Critical Evaluation of Experimental Data. *J. Chem. Eng. Data* **1994**, *39*, 876–886.

(32) Watson, W.; Zéberg-Mikkelsen, C. K.; Baylaucq, A.; Boned, C. High-pressure Density Measurements for the Binary System Ethanol+Heptane. *J. Chem. Eng. Data* **2006**, *51*, 112–118.

(33) Aparicio, S.; Alcarde, R.; Dávila, M. J.; García, B.; Leal, M. J. Properties of 1,8-Cineole: A Thermophysical and Theoretical Study. *J. Phys. Chem. B.* **2007**, *11*, 3167–3177.

(34) Alfaro, P.; Domínguez, M.; Teruel, M. I.; Urieta, J. S.; Mainar, A. M. Comportamiento Termodinámico de Componentes de Aceites Esenciales con Alcoholes: V^E y H^E de las Mezclas 1,8-Cineol+Etanol, 1,8-Cineol+1-Propanol. XXX Reunión Bienal de la Sociedad Española de Física, 2005.

(35) Sharma, S.; Patel, P. B.; Patel, R. S.; Patel, R. G.; Vora, J. J. Densities and Refractive Indexes of Binary Liquid Mixtures of Eucalyptol with some Alcohols. *J. Indian Chem. Soc.* **2007**, *84*, 807–812.

(36) Cibulka, I.; Hdnedkovsky, L. Liquid Densities at Elevated Pressures of n-Alkanes from C-5 to C-16: A Critical Evaluation of Experimental Data. *J. Chem. Eng. Data* **1996**, *41*, 657–668.

(37) Rowlinson, J. S.; Swinton, F. L. *Liquid and Liquid Mixtures*; Butterworths: London, 1982.

(38) Cerdeiriña, C. A.; Tovar, C. A.; González-Salgado, D.; Carballo, E.; Romaní, L. Isobaric Thermal Expansivity and Thermophysical Characterization of Liquids and Liquid Mixtures. *Phys. Chem. Chem. Phys.* **2001**, *3*, 5230–5236.

(39) Vallés, C.; Pérez, E.; Mainar, A. M.; Santafé, J.; Domínguez, M. Excess Enthalpy, Density, Speed of Sound, and Viscosity for 2-Methyltetrahydrofuran+1-Butanol at (283.15, 298.15, and 313.15) K. *J. Chem. Eng. Data* **2006**, *51*, 1105–1109.

(40) Joback, K. G.; Reid, R. C. Estimation of Pure Component Properties of Pure Components from Group Contributions. *Chem. Eng. Commun.* **1987**, *57*, 233–243.

(41) Lee, B. I.; Kesler, M. G. Generalized Thermodynamic Correlation Based on 3-Parameter Corresponding States. *AIChE J.* **1975**, *21*, 510–527.

(42) Stull, D. Vapor Pressure of Pure Substances-Organic Compounds. *Ind. Eng Chem.* **1947**, *39*, 517–540.

(43) Farelo, F.; Santos, F.; Serrano, L. Isobaric Vapor Liquid Equilibrium nn Binary Mixtures of a-Pinene, Limonene and 1,8-Cineole. *Can. J. Chem. Eng.* **1991**, *69*, 794–799.

(44) Daubert, T. E.; Danner, R. P. *Physical and Thermodynamic Properties of Pure Compounds: Data Compilation*; Hemisphere: NY, 1989.

(45) Pfohl, O.; Petkov, S.; Brunner, G. "PE" Quickly Makes Available the Newest Equations of State Via the Internet. *Ind. Eng. Chem. Res.* **2000**, *39* (11), 4439–4440.

(46) Wertheim, M. S. Fluids with Highly Directional Attractive Forces. 1. Statistical Thermodynamics. *J. Stat. Phys.* **1984**, *35*, 19–34.

(47) Wertheim, M. S. Fluids with Highly Directional Attractive Forces. 2. Thermodynamic Perturbation-Theory and Integral Equations. *J. Stat. Phys.* **1984**, *35*, 35–47.

(48) Wertheim, M. S. Fluids with Highly Directional Attractive Forces. 3. Multiple Attraction Sites. *J. Stat. Phys.* **1986**, *42*, 459–476.

(49) Wertheim, M. S. Fluids with Highly Directional Attractive Forces.4. Equilibrium Polymerization. *J. Stat. Phys.* **1986**, *42*, 477–492.

(50) Chen, S. S.; Kreglewski, A. Applications of Augmented an der Wals Theory of Fluids. 1. Pure Liquids. *Ber. Bunsen-Ges.* **1977**, *81* (10), 1048–1052.

(51) Barker, J. A.; Henderson, D. Perturbation Theory and Equation of State for Fluids. 2. A Successful Theory of Liquids. *J. Chem. Phys.* **1967**, *47* (11), 4714–4721.

(52) Riddick, J. A.; Bunger, W. B.; Sakano, T. K. *Organic Solvents, Techniques of Chemistry*, 4th ed.; Wiley-Interscience: New York, 1986; *Vol. II*.

Received for review January 9, 2008. Accepted February 29, 2008. The authors thank the financial support of MEC (Project CTQ2006-CO2-02). E. Langa thanks GATHERS Group for her research position. L. Martin thanks I3A for a junior research fellowship and MEC for the FPU grant (ref AP2006-2054).

JE800024U